The *miR-424(322)/503* cluster orchestrates remodeling of the epithelium in the involuting mammary gland

David Llobet-Navas,[1,2,3,14] Ruth Rodríguez-Barrueco,[1,2,3,14] Verónica Castro,[1,2] Alejandro P. Ugalde,[4] Pavel Sumazin,[5,6,7] Damian Jacob-Sendler,[1,2] Berna Demircan,[8] Mireia Castillo-Martín,[3] Preeti Putcha,[1,2] Netonia Marshall,[1,2] Patricia Villagrasa,[1,2] Joseph Chan,[5,6,7] Félix Sanchez-Garcia,[5,6,7,9] Dana Pe'er,[5,6,7,9] Raul Rabadán,[5,6,7] Antonio Iavarone,[1,2] Carlos Cordón-Cardó,[3] Andrea Califano,[1,2,7,10] Carlos López-Otín,[4] Elena Ezhkova,[11,12,13] and Jose M. Silva[1,2,3,15]

[1]Institute for Cancer Genetics, Department of Pathology, Columbia University, New York, New York 10032, USA; [2]Irving Cancer Research Center, Columbia University, New York, New York 10032, USA; [3]Department of Pathology, Icahn School of Medicine at Mount Sinai, New York, New York 10029, USA; [4]Departamento de Bioquímica y Biología Molecular, Instituto Universitario de Oncología, Universidad de Oviedo, Oviedo 33006, Spain; [5]Columbia Initiative in Systems Biology, Columbia University, New York, New York 10032, USA; [6]Center for Computational Biology and Bioinformatics, Irving Cancer Research Center, Columbia University, New York, New York 10032, USA; [7]Department of Biomedical Informatics, Columbia University, New York, New York 10032, USA; [8]Faculty of Medicine, Istanbul Medeniyet University, Istanbul 34700, Turkey; [9]Department of Biological Sciences, Columbia University, New York, New York 10027, USA; [10]Department of Biochemistry and Molecular Biophysics, Columbia University, New York, New York 10032, USA; [11]Black Family Stem Cell Institute, [12]Department of Development and Regenerative Medicine, Icahn School of Medicine at Mount Sinai, Mount Sinai School of Medicine, New York, New York 10029, USA; [13]Stem Cell Institute, Mount Sinai School of Medicine, New York, New York 10029, USA

The mammary gland is a very dynamic organ that undergoes continuous remodeling. The critical regulators of this process are not fully understood. Here we identify the microRNA cluster *miR-424(322)/503* as an important regulator of epithelial involution after pregnancy. Through the generation of a knockout mouse model, we found that regression of the secretory acini of the mammary gland was compromised in the absence of *miR-424(322)/503*. Mechanistically, we show that *miR-424(322)/503* orchestrates cell life and death decisions by targeting *BCL-2* and *IGF1R* (insulin growth factor-1 receptor). Furthermore, we demonstrate that the expression of this microRNA cluster is regulated by TGF-β, a well-characterized regulator of mammary involution. Overall, our data suggest a model in which activation of the TGF-β pathway after weaning induces the transcription of *miR-424(322)/503*, which in turn down-regulates the expression of key genes. Here, we unveil a previously unknown, multilayered regulation of epithelial tissue remodeling coordinated by the microRNA cluster *miR-424(322)/503*.

[*Keywords*: BCL2; IGF1R; TGFβ; mammary gland development; *miR-424*; *miR-503*]

Supplemental material is available for this article.

Received January 2, 2014; revised version accepted February 19, 2014.

The mammary gland is a very dynamic organ that passes through continuous tissue remodeling during the female lifetime (Howard and Gusterson 2000; Ip and Asch 2000; Macias and Hinck 2012). The appearances of distinct placodes containing mammary epithelial precursors initiate the limited ingrowth of a rudimentary ductal tree during embryogenesis that undergoes extensive expansion at puberty in the female breast. In adult females, side branches and lobulo–alveolar structures are in a continuous cycle in response to the cycling ovarian hormones. During pregnancy, secretory alveoli develop in response to specialized hormones, forming a very dense lactiferous epithelial tree that invades almost the entire mammary fat pad. During weaning, regression of this architecture occurs, leading to alveoli and secretory duct collapse (a process known as involution).

[14]These authors contributed equally to this work.
[15]Corresponding author
E-mail jose.silva@mssm.edu
Article published online ahead of print. Article and publication date are online at http://www.genesdev.org/cgi/doi/10.1101/gad.237404.114.

During the last two decades, key details about the molecular mechanism and regulation of the massive remodeling that occurs during mammary gland involution have emerged (Watson 2006; Stein et al. 2007; Watson and Kreuzaler 2011). It is well established that involution occurs in two distinct phases according to its reversibility. The first 48 h after weaning are characterized by apoptotic cell death without changes in acini architecture. Molecularly, this step involves both the intrinsic and the extrinsic apoptotic pathways and is modulated by the expression levels of members of the pro- and anti-apoptotic BCL-2 family. A few signaling pathways have been identified as upstream modulators of apoptosis, some of the most relevant being TGF-β, IGF (insulin growth factor), LIF, NF-κB, and STAT-3. Cues for these pathways converge to regulate Akt/PKB, which in turn balances cell life and death decisions. The second phase, 2 d after initiation of involution, is characterized by the collapse of the alveolar structure and degradation of the supportive extracellular matrix, which is mediated by metalloproteases.

Despite our current knowledge of mammary gland development, our understanding of the contribution of miRNAs to this process is in its infancy. MicroRNAs (miRNAs) are small noncoding RNAs, ~22 nucleotides (nt) in length, with critical roles in multiple aspects of cell biology and organism physiology (Bartel 2004, 2009). miRNAs post-transcriptionally regulate gene expression mainly by targeting mRNAs for cleavage, translational repression, and mRNA destabilization. A very limited number of studies have identified and validated miRNAs with a role in any aspect of normal mammary gland biology (Avril-Sassen et al. 2009; Tanaka et al. 2009; Ucar et al. 2010; Yang et al. 2010; Cui et al. 2011; Le Guillou et al. 2012), and even fewer have studied their function in vivo (Ucar et al. 2010; Le Guillou et al. 2012).

Here we identified the *miR-424(322)/503* cluster as an important regulator of involution. To investigate the processes influenced by this cluster in vivo, we generated a knockout mouse model in which *miR-424(322)/503* was deleted. Although knockout mice were fully viable, detailed analyses of mammary gland development revealed a delayed pattern of involution after pregnancy. The study of *miR-424(322)/503* targets identified a group of genes with a key role in apoptosis (*BCL-2*) and insulin signaling (*IGF1R* [IGF-1 receptor]). Importantly, we also demonstrated that the changes in the expression of these targets mediated by the *miR-424(322)/503* cluster impact cell death as well as the activity of key signal transduction pathways (AKT and ERK1/2) in vitro and in vivo. Furthermore, our studies linked the expression of the cluster to TGF-β, which plays a well-known role in mammary gland involution (Faure et al. 2000; Nguyen and Pollard 2000; Stein et al. 2007). Overall, our studies suggest a model in which the expression of a primary transcript containing the *miR-424(322)/503* cluster is up-regulated during involution via TGF-β exposure. Once processed, these mature miRNAs are part of the mechanisms that induce involution by down-regulating the expression of key components of signal transduction and cell death.

Results

The miRNA cluster 424(322)/503 *is up-regulated during mammary gland involution in mammary epithelial cells*

In order to investigate the landscape of miRNAs expressed in the mammary gland epithelium, we performed miRNA high-throughput sequencing (HTP-seq) studies on six different stages of development (puberty, estrus, diestrus, pregnancy [15 d], lactation [10 d], and involution [3 d]) (Fig. 1A). Estrus and diestrus represent the two most different stages that occur during periodic ovarian cycles. Estrus is characterized by the presence of primary and secondary epithelial ducts with very little alveolar budding. On the other hand, the diestrus stage is characterized by a higher abundance of alveolar buds. Involution of the mammary gland after pregnancy is the phase where the most dramatic changes occur. We thus decided to investigate the miRNAs that were specifically expressed in the mammary epithelial cells during this period. Of 1281 described mature miRNA sequences (miRBase release-19), ~200 were expressed in at least one developmental stage (complete miRNA profile will be reported elsewhere) (data not shown). When we searched for miRNAs preferentially up-regulated during involution, we found a group of 12 miRNAs with a Z-score ≥ 1.5 (Fig. 1A). Additionally, we studied by quantitative RT–PCR (qRT–PCR) the expression of these miRNAs across a series of 15 different organs. Interestingly, *miR-424(322)* was expressed at the highest levels almost exclusively in involuting mammary epithelium, while the rest of the miRNAs in the list were expressed at higher levels in several other organs (Fig. 1B). Furthermore, *miR-424(322)* was also the most up-regulated miRNA transitioning from lactation to involution (72 h) (Fig. 1C). Nine of the 12 miRNAs that we found preferentially up-regulated during involution have been previously studied during mammary development (Avril-Sassen et al. 2009). While we used HTP-seq of purified mammary epithelial cells to evaluate miRNA expression, the Avril-Sassen et al. (2009) study used a bead-based flow cytometric microarray platform and whole mammary gland RNA extraction without purification. This difference complicates the direct comparison of the data; however, we noticed that six of the nine overlapping miRNAs between both studies showed similar expression patterns (Supplemental Fig. S1A).

miR-424(322) belongs to the *miR-16* family (Liu et al. 2008; Finnerty et al. 2010). Some members of this miRNA family have been previously shown to target known modulators of cell cycle and apoptosis, which are fundamental pathways during involution. We observed that other members of the *miR-16* family were expressed in the mammary epithelium; however, their steady-state levels did not increase significantly during involution (72 h) (Supplemental Fig. S1B). Remarkably, evolutionary studies on the *miR-16* family have revealed that while all vertebrates studied to date express *miR-15a*, *miR-15b*, *miR-16*, *miR-103*, and *miR-107*, only mammals are known to express *miR-195*, *miR-424(322)*, *miR-497*, *miR-503*, and

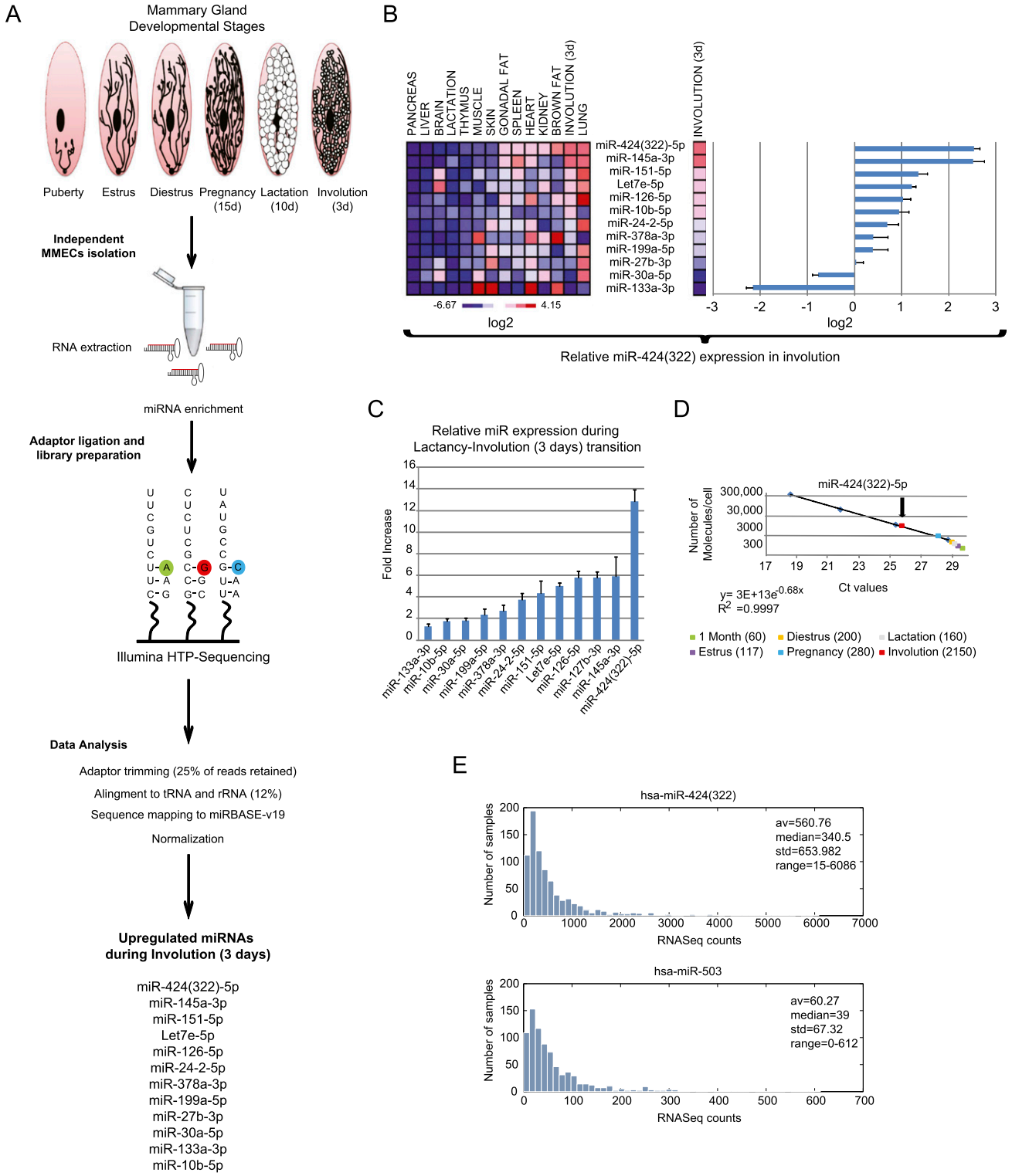

Figure 1. Up-regulation of the miRNA cluster *424(322)/503* in the epithelium during the involution of the mammary gland. (*A*) Schematic representation of the strategy performed to identify stage-specific miRNAs in the epithelium of the mammary gland and lists of miRNAs differentially up-regulated during involution. Samples were collected at puberty (1 mo), estrus, diestrus, pregnancy (15 d), lactation (10 d), and involution (3 d). (*B*) Tissue-specific expression analysis of involution-related miRNAs and their relative expression in the involuting mammary epithelium; $n = 5$. (*C*) Fold up-regulation of involution-related miRNAs when compared with lactating mammary glands; $n = 5$. (*D*) Estimation of the number of molecules of *miR-322* per cell during mammary gland development; $n = 3$. (*E*) Distribution of the normalized number of reads of *miR-424(322)* and *miR-503* per sample after miRNA HTP-seq analysis in a cohort of 800 primary breast tumors (The Cancer Genome Atlas [TCGA] breast cancer). See also Supplemental Figure S1.

miR-646 (Finnerty et al. 2010), suggesting a specialized function.

Prompted by these data, we decided to investigate in more detail the role and regulation of *miR-424(322)* in the remodeling of involuting mammary epithelium. A more detailed analysis of the expression of the mature *miR-424(322)* during early (24 h after weaning) and late (3 d after weaning) involution confirmed that it peaks during late involution (Supplemental Fig. S1C). *miR-424(322)* is located in chromosome X and in close proximity (~380 base pairs [bp]) to *miR-503* in both humans and mice. Both miRNAs have been proposed to be expressed as a cluster (Forrest et al. 2010), and, in fact, we were able to retrotranscribe a transcript containing both miRNAs (Supplemental Fig. S1D). Interestingly, *miR-503* was filtered out in our HTP-seq analysis because of its low expression levels, suggesting that *miR-424(322)* is preferentially processed from the precursor miRNA (pre-miRNA). By titrating chemically synthesized mature miRNAs, we estimated that the number of molecules of mature *miR-322* is about a few hundred per cell but increases to a few thousand (fivefold to 10-fold) during involution (Fig. 1D; Supplemental Fig. S1E). Although the mature form of *miR-503* also increased proportionally during involution, the steady-state levels of *miR-503* were about a log of magnitude lower than levels of *miR-322* (Supplemental Fig. S1F). By comparing the number of reads corresponding to both miRNAs in the HTP-seq data generated by The Cancer Genome Atlas (TCGA) breast cancer study from >800 samples (Fig. 1E; https://tcga-data.nci.nih.gov/tcga), we also confirmed that higher levels of *miR-424(322)* are maintained in humans. Finally, HTP-seq data available in the miRBase database (http://www.mirbase.org) as well as published studies in normal ovarian tissue (Ahn et al. 2010) confirmed a comparable relative *miR-424(322)/miR-503* ratio of expression. Taken together, these data suggest that higher levels of mature *miR-424(322)* compared with *miR-503* are well preserved between humans and mice. The reason for the unbiased levels between these two miRNAs is unclear. In this regard, it has been previously reported that *miR-503* is usually unstable and that this instability is mediated by the seed region and the 3′ end (Rissland et al. 2011).

miR-424(322)/503 *knockout mice present defects in mammary gland involution and display alveoli hyperplasia after pregnancy*

To study the role of the *miR-424(322)/503* in the mammary epithelium, we generated a knockout mouse model using zinc finger nuclease (ZFN; Sigma) technology (Fig. 2A; Urnov et al. 2010). Two ZFNs cutting upstream of and downstream from the cluster were engineered and injected into 400 fertilized oocytes. These oocytes were injected into recipient C57BL/6 females, and 54 viable pups were born. Males and females were born at a Mendelian ratio. The genotype of these animals revealed that 50% of the males carried a mutated *miR-322/503* allele. In females, 30% were heterozygous, and 8.3% had both alleles mutated. Due to the nature of the mechanisms involved in the repair of the double-strand breaks generated by the ZNFs, there were varying sizes of the deletion in mutant alleles. These deletions ranged from 22 nt to larger fragments of almost 1 kb containing the two miRNAs (Supplemental Fig. S2A,B). For our studies, we used mice containing deletions of both mature miRNAs (alleles *7A* and *38*) (Fig. 2A). As expected, both knockout alleles showed the same phenotype (see below). Consequently, in this study and for simplification, we do not make any distinction between them and use the general term *miR-424(322)/503* knockout. We also obtained alleles where only one of the two miRNAs was deleted. Interestingly, when we analyzed the expression levels of the remaining miRNA, we observed that these levels were severely reduced to barely detectable levels (Fig. 2B). This result suggests that the sequence/structure of the *miR-424(322)/503* primary transcript is essential for proper generation of mature miRNAs.

Phenotypically, knockout pups were identical to the wild type in appearance, size, and weight. We did not observe any evident differences between knockout and wild-type animals during the first 2 mo of life. At a later age, knockout mice presented with a higher body weight due to increased white fat content (characterization of this phenotype will be reported elsewhere).

Next, we concentrated our studies on the mammary gland epithelium during the different phases of development. A systematic study of the female epithelial mammary tree was done by comparing whole-mount preparations stained with carmine red and quantifying the area occupied by epithelial cells and adipocytes (Chapman et al. 1999; Tiffen et al. 2008). Acini morphology and organization were studied using hematoxyilin/eosin (H&E) staining, and basal (cytokeratin 5) and luminal (cytokeratin 18) markers were studied using immunohistological techniques. These studies revealed no major differences in the organization (size, length, number, and basal/luminal marker distribution) of the ducts and lobules during puberty and during estrus/diestrus of nulliparous animals at an early age (up to 3 mo) (Supplemental Fig. S2C–E). Older virgin knockout females presented a few slightly enlarged terminal ductal lobular units (TDLUs) containing two to three times more acini than age-matched wild-type counterparts (Fig. 2C). Interestingly, parous females displayed mammary glands with multifocal, larger TDLUs compatible with alveoli hyperplasia (Fig. 2D).

Expression of the *miR-424(322)/503* cluster increases during involution after pregnancy. Thus, it is plausible that the observed phenotype in parous animals has its origin at this stage. Our studies during pregnancy and involution revealed that during pregnancy, secretory acini in knockout animals displayed normal morphological and functional (milk-producing) characteristics (Supplemental Fig. S2F,G). In addition, we also observed comparable morphological features at early involution (24 h after weaning) between knockout and wild-type animals (Supplemental Fig. S2H,I). At late involution (3 d after weaning), wild-type females displayed massive destruction of the lobular epithelium, which led to the absence of

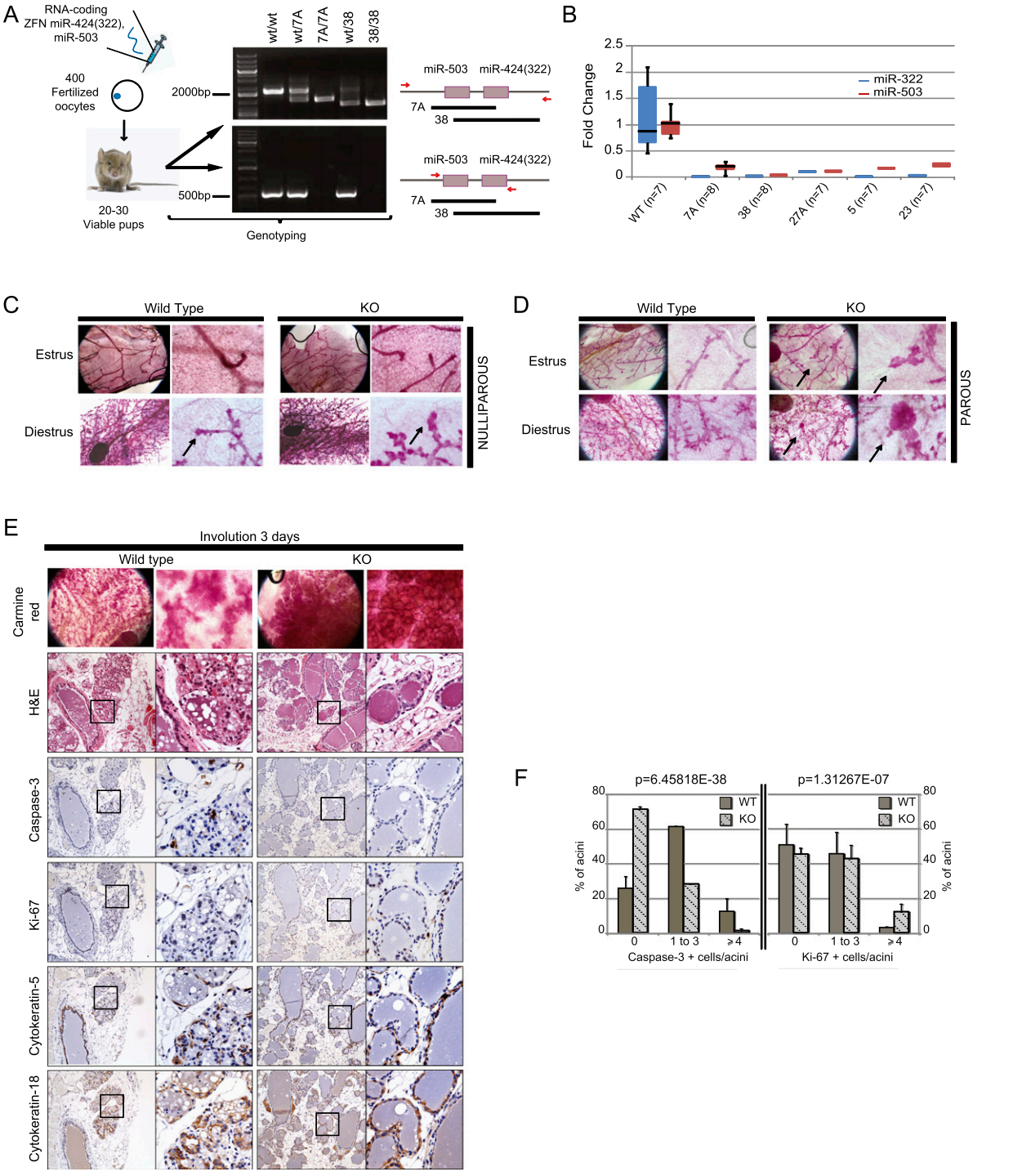

Figure 2. *miR-424(322)*$^{-/-}$*/503*$^{-/-}$ knockout (KO) mice show delayed post-lactation mammary gland involution and alveolar hyperplasia. (*A*) Modeling of *miR-424(322)*$^{-/-}$*/503*$^{-/-}$ double-knockout mice by using the ZFN technology generates multiple deleted alleles. (*B*) qRT–PCR expression values for *miR-424(322)* and *miR-503* in wild-type animals and *miR-424(322)*$^{-/-}$*/503*$^{-/-}$ knockout mice with different deleted alleles. (*C*) Representative carmine red staining performed on old nulliparous female mammary glands reveals discrete enlarged terminal ductal lobular units (TDLUs). (*D*) In parous females, TDLUs progress into enlarged multifocal structures compatible with alveolar hyperplasia. (*E*) Representative stainings of involuting mammary glands at 72 h. H&E, cytokeratin 5, cytokeratin 18, and caspase-3 stainings reveal drastic lobular epithelium death in wild-type (WT) mice, while the mammary epithelium of *miR-424(322)/503* knockout animals still presents well-organized and structured acini. (*F*) The graph shows quantification of caspase-3-positive cells per acini for immunostainings (between 80 and 150 acini were counted per condition). See also Supplemental Figure S2.

recognizable acini structures; in contrast, knockout females presented lobules with morphologically well-structured acini (Fig. 2E; Supplemental Fig. S2H,I). Remarkably, apoptosis was reduced 3 d after weaning in knockout animals, as indicated by fewer cells displaying activated caspase-3 immunostaining (Fig. 2E,F; Supplemental Fig. S2J).

It is important to mention that both knockout alleles (*7A* and *38*) were crossed with wild-type animals for six generations (a 98.5% clean background) to confirm the association between the genotype *miR-424(322)/503* knockout and the phenotype. As expected, the phenotype segregated with the knockout alleles.

The miRNA cluster 424(322)/503 *targets the key regulators of mammary gland involution, BCL-2 and IGF1R*

The biological functions of miRNAs are mediated by their ability to attenuate the expression of targeted mRNAs. Thus, we investigated the targets of the *miR-424(322)/503* cluster. Computational prediction of targets based on seed sequence conservation (Lewis et al. 2005) as well as nonconserved sites (Grimson et al. 2007) is a widely used strategy to identify miRNA targets. We used the TargetScan algorithm (http://www.targetscan.org), which has been shown to have one of the highest specificities in preselecting putative target genes (Shirdel et al. 2011). *miR-424(322)* and *miR-503* have almost identical seed sequences and belong to the same miRNA family (Fig. 3A). Thus, it is not surprising that the predicted target overlap between both miRNAs is very high [>90% of the predicted targets conserved in mammals for *miR-503* are included in the list for *miR-424(322)*] (Supplemental Fig. S3A). Computational predictions of miRNA targets result in hundreds, if not thousands, of candidates. In order to reduce this number of genes, we exploited the fact that up-regulation of the targeting miRNA reduced the expression level of targets with potent binding side sequences (Bartel 2009; Guo et al. 2010). We transduced MCF-10A, an immortalized but nontransformed human mammary epithelial cell (HMEC) line, with lentiviruses expressing the miR cluster or a control vector and compared their expression profiles after 48 h. As expected, this study showed a strong statistically significant reduction in the expression of predicted target genes ($P < 10^{-34}$) (Fig. 3B). Pathway analysis (Ingenuity) of the predicted targets that showed reduction in mRNA levels identified a group of genes involved in cell cycle, apoptosis, TGF-β, and canonical ERK/AKT signal transduction pathways (Supplemental Fig. S3B,C). Since these pathways are key regulators of mammary gland involution (Neuenschwander et al. 1996; Nguyen and Pollard 2000; Schwertfeger et al. 2001; Stein et al. 2007; Macias and Hinck 2012), we decided to further study a series of these putative targets by following a systematic approach.

First, we assessed the ability of the predicted target sites of these genes to regulate the expression of a reporter gene. We cloned a portion of the untranslated regions (UTRs) containing the predicted miR cluster-binding sites for 20 genes related to the above-mentioned pathways downstream from a luciferase reporter gene (Luc-UTR). We then cotransduced 293T cells with the corresponding Luc-UTR reporter, a renilla luciferase expression vector lacking any UTR used for normalization purposes, and a plasmid expressing the *miR-424(322)/503* cluster. The UTRs of 14 out of 20 candidates showed a statistically significant reduction of the Luc-UTR reporter in the presence of the construct expressing the *miR-424(322)/503* cluster (Fig. 3C).

Next, we performed additional validation using photoactivatable ribonucleoside-enhanced cross-linking immunoprecipitation (PAR-CLIP) of the RNA-induced silencing complex (RISC) (Hafner et al. 2010). PAR-CLIP experiments were performed in MCF-10A control cells and an MCF-10A variant transduced with lentivirus vector expressing the *miR-424(322)/503*. After CLIP, qRT–PCR was used to quantify the levels of captured mRNA for the 14 selected targets. Our data revealed a statistically significant enrichment for six of 14 targets, four of them showing more than twofold enrichment (*CDC25A*, *BCL-2*, *IGF1R*, and *CCNE1*) (Fig. 3D). Interestingly, there was a positive correlation between the enrichment in the PAR-CLIP assay and the Luc-UTR reporter assay. Because the expression of *BCL-2* (Metcalfe et al. 1999) and *IGF1R* (Modha et al. 2004) has been found to be down-regulated during involution and because apoptosis and insulin signaling are well-known regulators of this process, we decided to further investigate these two genes. Additionally, we also studied *CCNE1*, as it has previously been shown to be targeted by this miR cluster. Thus, we next mutated the predicted conserved *miR-424(322)/503*-binding sites in the Luc-UTR constructs for these three genes. Modification of the sequence complementary to the miRNA seed region in the mRNA UTR reverted completely the reduction of luciferase signal after up-regulation of the *miR-424(322)/503* cluster (Fig. 3E).

Next, we analyzed the impact of the *miR-424(322)/503* on the levels of the endogenous proteins. In order to use the most biologically relevant model, we engineered a MCF-10A variant to up-regulate the expression of the miRNA-424(322)/503 using a doxycycline (Dox)-inducible system [MCF-10A-*424(322)/503miR*-Dox]. Importantly, this system allowed us to up-regulate *miR-424(322)* and *miR-503* to levels comparable with those observed in involuting mouse mammary epithelial cells (MMECs) (Supplemental Fig. S3D). Up-regulation of the miR cluster in MCF-10A-*424(322)/503miR*-Dox clearly attenuated the expression levels of BCL-2 and IGF1R, but the effect on CCNE1 expression was modest (Fig. 3F). Finally, we studied the expression levels of these three targets in primary MMECs during development as well as in telomerase (Tert)-immortalized mammary epithelial cell lines from wild-type and knockout animals. Western blot studies revealed an evident down-regulation of Igf1r and Bcl-2 during involution that occurs at the highest peak of the mature *miR-424(322)* and *miR-503* expression, while no major effect was seen in Ccne1 (Fig. 3G; Supplemental Fig. S3E). Remarkably, both primary involuting MMECs and Tert-immortalized *miR-424(322)/503* knockout mammary

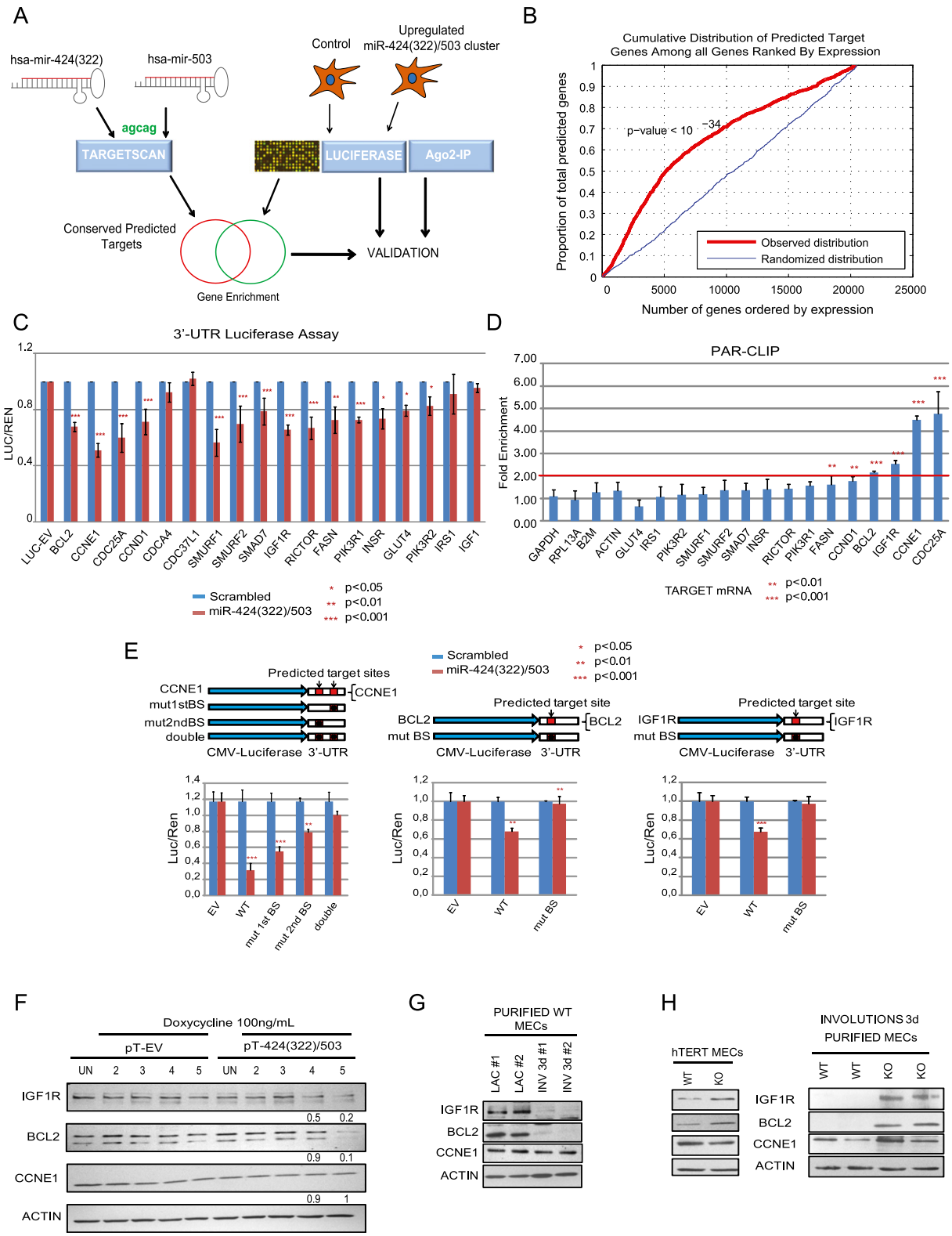

Figure 3. *BCL2* and *IGF1R* are bona fide targets of *miR-424(322)/503*. (*A*) The illustration represents the multistep strategy designed to identify *miR-424(322)/503* targets. (*B*) Cumulative distribution of predicted *miR-424(322)/503* targets and nontargets when their expression levels from control and *miR-424(322)/503*-up-regulated MCF-10A cells are compared. (*C*) Cloning of the 3′ UTR and subsequent 3′ UTR-luciferase assays of the selected candidates shows differential targeting activity by *miR-424(322)/503* ($n = 5$) that was further filtered by PAR-CLIP expression analysis via qRT–PCR ($n = 5$; shown in *D*). (*E*) miRNA-binding site mutagenesis and luciferase assays were performed in the most relevant candidates to prove the *miR-424(322)/503*-binding specificity. (*F*) MCF-10A cells were lentivirally transduced with an inducible plasmid expressing the *miR-424(322)/503* and treated with Dox for 5 d. Western blot analysis showed a decrease in the endogenous protein levels of *miR-424(322)/503* targets IGF1R2 and BCL2 but not in CCNE1 ($n = 5$). (*G*) Western blot studies of purified mouse mammary epithelium show that IGF1R and BCL2 protein levels decrease during the transition from lactation to involution in wild-type (WT) animals and that post-lactation *miR-424(322)/503* knockout animals as well as Tert-immortalized *miR-424(322)/503* knockout cells (Tert-KO) present higher expression of these targets than their wild-type counterparts (shown in *H*). A minimum number of five animals were analyzed. See also Supplemental Figure S3.

epithelial cells presented consistently higher protein levels of these proteins than wild-type counterparts. Again no significant changes were observed in Ccne1 (Fig. 3H).

Expression of the miR-424(322)/503 *cluster modulates IGF-1 signal transduction and apoptosis*

While the data described above clearly showed the ability of *miR-424(322)/503* to modulate the expression of *BCL-2* and *IGF1R*, it was crucial to determine whether this regulation was biologically relevant.

IGF1R is the bona fide receptor for IGF-1 (Pollak 2012). IGF-1 binding activates the receptor kinase, leading to autophosphorylation and phosphorylation of downstream substrates and resulting in the activation of two main signaling pathways, the PI3K–AKT/PKB and the Ras–MAPK pathways. To test the role of *miR-424(322)/503* in these pathways, IGF-1 was added to starved MCF-10A-*424(322)/503miR*-Dox cells after the miR cluster was induced by the addition of Dox to the medium. Down-regulation of IGF1R protein levels mediated by induction of the miR cluster led to a weaker response to IGF-1 stimulation, as demonstrated by reduction in the levels of phospho-IGF1R (Tyr1135 and Tyr1131), phospho-AKT (Ser473), and phospho-ERK1/2 (Thr202/Tyr204) (Fig. 4A). Importantly, wild-type phosphorylation levels in all three proteins were restored when a nontargetable version of *IGF1R* lacking the 3′ UTR was exogenously expressed (Fig. 4B; Supplemental Fig. S4A). To complement our studies, we performed a similar analysis with Tert-immortalized MMECs and primary MMECs. These revealed that *miR-424(322)/503* knockout cells, which present higher levels of Igf1r, were more sensitive to IGF-1 stimulation than their wild-type counterparts (Fig. 4C,D). Altogether, these data demonstrate that modulation of *IGF1R* by *miR-424(322)/503* affects the response to IGF-1 and its downstream canonical signaling.

BCL-2 is the founding member of the Bcl-2 family of apoptosis regulator proteins (Colitti 2012), and its key role in the intrinsic apoptosis pathway is well established. BCL-2's prosurvival abilities are largely due to its ability to control mitochondrial membrane permeability by inhibiting proapoptotic proteins. Thus, we tested whether the ability to undergo apoptosis was affected by the *miR-424(322)/503* cluster. Apoptosis in MCF-10A-*424(322)/503miR*-Dox cells was induced by exposure to different chemotherapeutic agents (cisplatin and paclitaxel). Up-regulation of the *miR-424(322)/503* cluster by addition of Dox significantly increased apoptosis induced by paclitaxel and cisplatin as shown by Annexin-V FACS analysis, caspase-3, and PARP cleavage, while no differences were observed in control cells (Fig. 4E; Supplemental Fig. S4B–D). Importantly, transduction of a *BCL-2* mRNA that lacks the 3′ UTR eliminated this effect (Fig. 4F; Supplemental Fig. S4E–H). As previously done for ERK/AKT signaling studies, we also studied the response to apoptotic stress in our Tert-immortalized MMECs. We found that *miR-424(322)/503* knockout cells, which present higher levels of Bcl-2, were significantly more resistant to apoptosis than wild-type counterparts (Fig. 4G; Supplemental Fig. S4I,J). Overall, these data demonstrate that modulation of *BCL-2* by the *miR-424(322)/503* cluster affects the stress-induced apoptotic response.

Characterization of the 424(322)/503 promoter pri-miR and its modulation by TGF-β

To mechanistically understand the regulation of the *miR-424(322)/503* in the mammary epithelium, we studied the genomic organization of the locus. As a first approach, we took advantage of the publicly available information contained in the University of California at Santa Cruz genome (UCSC) browser (http://genome.ucsc.edu). The close proximity between *miR-424(322)* and *miR-503* suggests that the primary transcript containing both miRNAs exists as a cluster. Interestingly, a noncoding RNA (*MGC16121*) is described in the reference sequence gene bank whose 5′ precisely matches the predicted sequence of the precursor of *miR-424(322)* [pre-*miR-424(322)*] after pre-miR has been excised by the nucleoprocessor complex from the primary transcript (Fig. 5A).

A review of the track displaying maps of chromatin states generated by the Broad Institute/Massachusetts General Hospital ENCODE group using chromatin immunoprecipitation (ChIP) and HTP-seq (ChIP-seq) revealed a region located ~2 kb upstream of the *miR-424/503* cluster and strongly enriched in histone marks related to an active promoter (H3K4me2, H3K4me3, H3K9ac, and H3K27ac) in HMECs (Fig. 5A). Specifically, there was enrichment in a histone mark associated with transcription elongation (H3K36me3) just after the termination of the active promoter marks and spanning ~5–6 kb in a region containing the miRNA cluster (Fig. 5A). Remarkably, a comparable histone mark pattern was also found in the majority of the cell lines analyzed, with the exception of B cells (Supplemental Fig. S5A). In embryonic stem cells, this putative promoter seems to be poised for active transcription, as it presents both active and negative histone marks (Supplemental Fig. S5B; Bernstein et al. 2006). Finally, FOX2 CLIP-seq (CLIP coupled with HTP-seq) used to study RNAs associated with the splicing regulator FOX2 showed that the H3K36me3-enriched region was, in fact, transcribed in the 5′–3′ orientation, consistent with a primary transcript starting at the putative promoter upstream of the miR cluster (Fig. 5A).

In order to obtain further insights regarding the transcriptional regulation of the locus, we searched for conserved sequence motifs in the putative promoter region (the ~2-kb region enriched in the above-mentioned histone marks). Multiple alignments of 28 vertebrate species and measurements of evolutionary conservation using a hidden Markov model-based method (phastCons) (Pollard et al. 2010) identified several motifs conserved in vertebrates and mammals (Fig. 5B). Interestingly, one of these motifs represented two *SMAD*-binding boxes (Fig. 5B; Johnson et al. 1999). *SMAD*s are bona fide components of the TGF-β and BMP pathways (Massague et al. 2005). Significantly, TGF-β ligands have well-known roles in epithelial mammary gland morphogenesis (Nguyen and Pollard 2000; Stein et al. 2007; Macias and Hinck 2012).

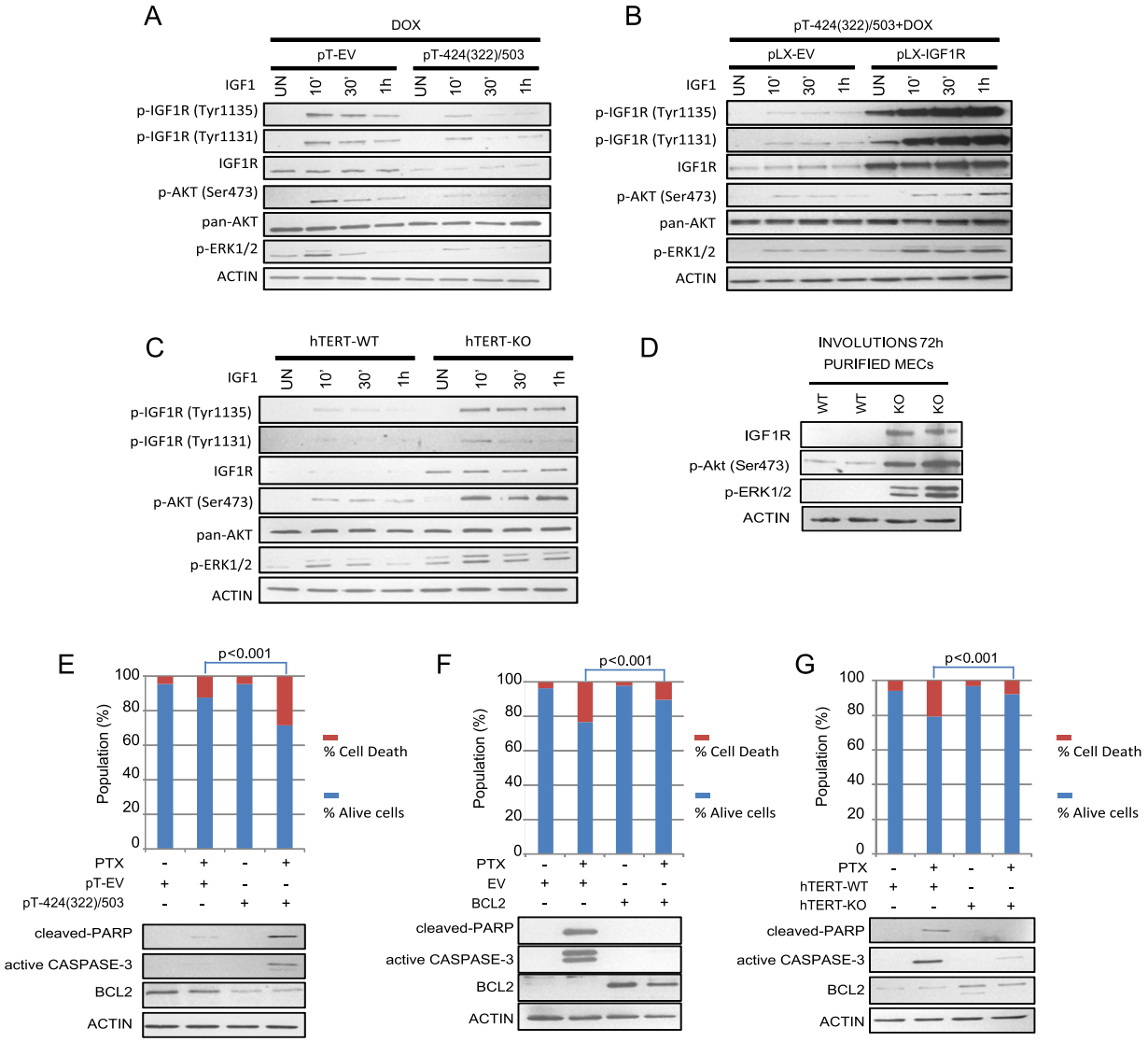

Figure 4. Induced *miR-424(322)/503* desensitizes cells to IGF-1 and primes cells to undergo apoptosis. (*A*) Dox-induced *miR-424(322)/503* targets endogenous IGF1R, causing desensitization to IGF-1 stimuli, as shown by Western blot. Cells were treated with Dox for 5 d, starved with 0.5% horse serum overnight, and subsequently treated with 50 ng/mL IGF-1 for the specified time points. (*B*) Engineered pT-424(322)/503 MCF-10A cells stably expressing a nontargetable form of *IGF1R* (pLX-*IGF1R*) are able to overcome IGF-1 desensitization caused by Dox-induced *miR-424(322)/503*. pLX-EV MCF-10A cells stably expressing an empty vector control. (*C*) Tert-immortalized knockout (Tert-KO) epithelial cells show consistent higher sensitivity to IGF-1 stimulation, as shown by Western blot. (*D*) Western blots showing increased activation of p-AKT and p-ERK in purified *miR-424(322)/503* knockout involuting mammary epithelial cells compared with their wild-type (WT) counterparts. (*E*) pT-424(322)/503 cells treated with Dox display higher sensitivity to apoptosis induced by 100 ng/mL paclitaxel (PTX) and 10 μg/mL cisplatin, as shown by quantification of cell death by Annexin-V staining and FACs analysis (*top* panel) and analysis of active caspase-3 and cleaved PARP by Western blot (*bottom* panel). MCF-10A cells were treated with Dox and subsequently exposed to PTX for 24 h. (*F*) Expression of a *BCL2* cDNA devoid of its 3′ UTR (pLOC-*BCL2*) blocks apoptotic cell death induced by PTX. (*G*) Tert-immortalized knockout cells exert higher resistance to PTX, as shown by Annexin-V, caspase-3, and PARP studies. All the experiments were performed in triplicate. See also Supplemental Figures S4 and S5.

Upon TGF-β ligand binding to its receptor, receptor-regulated SMAD-2 and SMAD-3 (R-SMADs) are activated by phosphorylation, heterodimerize with SMAD-4, and are then shuttled to the nucleus, where they act as transcription factors. R-SMADs are weak transcriptional activators and commonly cooperate with additional transcriptional modulators, such as E2Fs (Massague et al. 2005). Remarkably, a highly conserved region containing two *E2F*-binding motifs is located in close proximity (~100 bases) downstream from the *SMAD-3*-binding site.

TGF-β ligands have a key role during mammary epithelial development, mainly as potent inhibitors of proliferation (Howard and Gusterson 2000; Macias and Hinck 2012). During involution, expression of TGF-β ligands in the mammary gland, especially TGF-β3, is induced as soon as 3 h after forced weaning, and levels of TGF-β3 continue

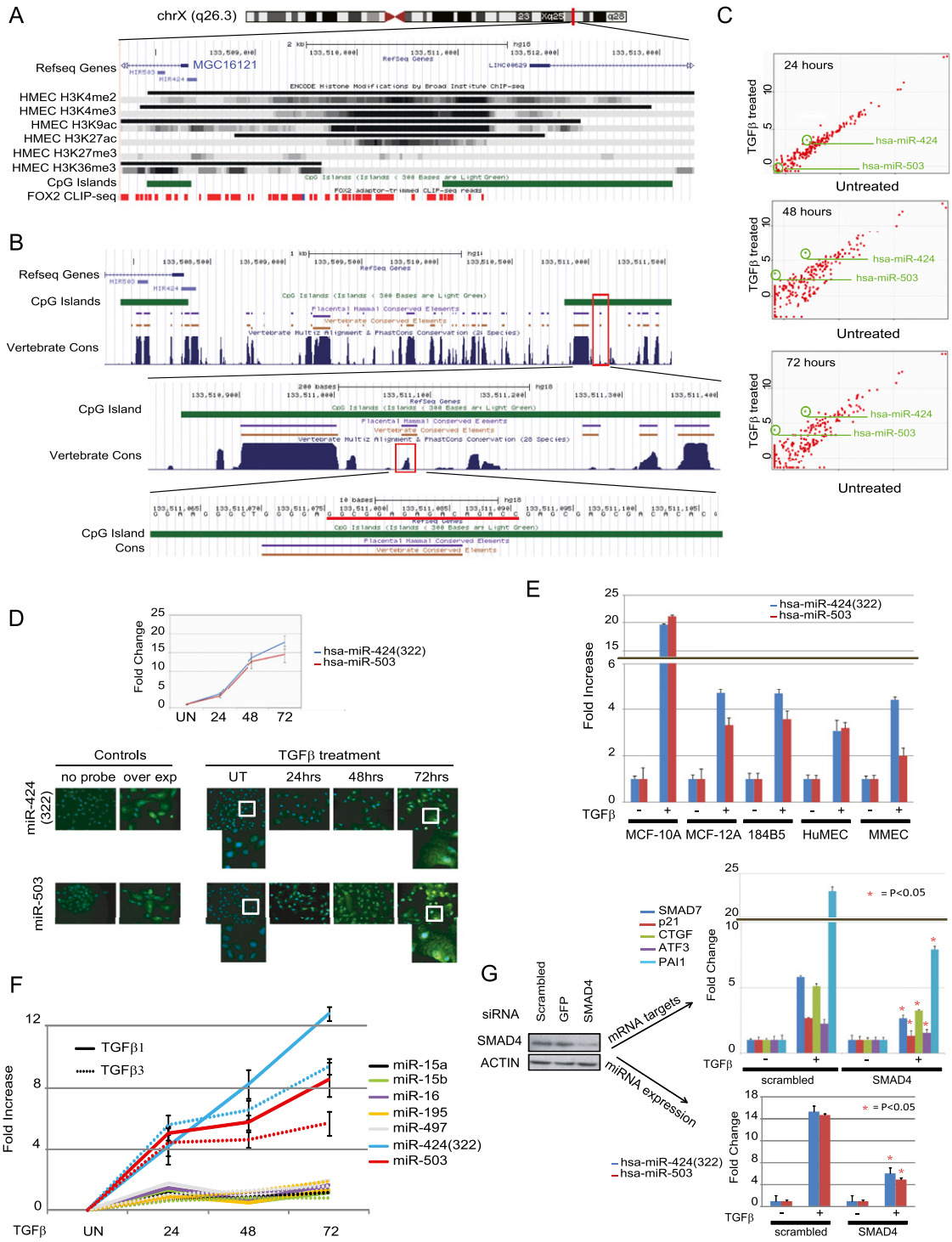

Figure 5. Genomic organization of *miR-424(322)/503* locus unveils transcriptional regulation mediated by TGF-β. (*A*) UCSC-extracted genomic locations of *miR-424(322)* and *miR-503* and putative regulatory elements located upstream in HMECs, including histone marks of transcriptionally active chromatin (H3K4me2, H3K4me3, H3K9ac, and H3K27ac), transcriptional silencing or repression (H3K27me3), and elongation (H3K36me3) as well as marks of elongation and splicing events, represented by genome-wide FOX2 CLIP-seq. The presence of additional regulatory regions such as CpG islands is also depicted. (*B*) Representation of the conservation status of *miR-424(322)*, *miR-503*, and the upstream regulatory regions using a vertebrate and placental mammal Markov model. Using this method, 28 vertebrate species were aligned to assess conservation status. Magnification of a small conserved region located upstream (highlighted in red) identifies two conserved *SMAD*-binding motifs. (*C*) Analysis by miRNA expression arrays of MCF-10A treated with 10ng/mL TGF-β for 24, 48, and 72 h. (*D*) Results were further validated by qRT–PCR (*top* panel) and in situ hybridization (*bottom* panel). For in situ hybridization, MCF-10A cells transduced with a construct expressing the cluster *miR-424(322)/503* were used as a positive control. (*E*) TGF-β-dependent regulation of *miR-424(322)* and *miR-503* was verified in other HMEC lines (MCF-12A and 184B5), HuMECs, and primary Tert-immortalized MMECs. Cells were treated with 10 ng/mL TGF-β1 for 48 h. (*F*) Expression analysis by qRT–PCR of *miR-15/16* family members in MCF-10A cells upon treatment with 10 ng/mL TGF-β for several days. (*G*) TGF-β-dependent *miR-424(322)* and *miR-503* expression was demonstrated by transfecting MCF10A cells with siRNA against SMAD4. Scrambled siRNAs and siRNAs against GFP were used as negative controls. The expression of bona fide TGF-β targets (*top* panel) and *miR-424(322)* and *miR-503* (*bottom* panel) was performed by qRT–PCR. See also Supplemental Figure S5.

to increase during the following hours to remain high for several days (Faure et al. 2000; Nguyen and Pollard 2000). Furthermore, expression of TGF-β type II receptor (Faure et al. 2000) and the nuclear internalization of Smad-4 (Nguyen and Pollard 2000) also occur in the mammary epithelium at about the same time. Although the role of TGF-β3 is not fully understood, in vivo evidence from transgenic mice expressing *Tgf*-β3 under the β-lactoglobin promoter or expressing a dominant-negative form of the *Tgf*-β receptor-II in the mammary gland (*MMTV-DNIIR*) as well as from animals where *Tgf*-β3 knockout mammary epithelial cells were orthotopically transplanted demonstrates the importance of *Tgf*-β signaling during the early and late involution phases (Nguyen and Pollard 2000; Gorska et al. 2003). Based on the above information, we hypothesized that exposure to TGF-β ligands during involution up-regulates the expression of *miR-424(322)/503*, which in turn modulates key players of cell cycle, apoptosis, and IGF-1 signaling.

The mammary cell line MCF-10A is a widely used model to study TGF-β response in mammary epithelial cells (Iavarone and Massague 1997; Karakas et al. 2006). Despite being null for the *INK4B* gene, these cells retain the ability to arrest after being exposed to TGF-β. (Iavarone and Massague 1997). To study the regulation of the *miR-424(322)/503* cluster, we exposed MCF-10A cells to TGF-β1 and, using miRNA microarrays, tracked the expression of 799 human miRNAs (Sanger miRbase release 10.1) through time. Both *miR-424(322)* and *miR-503* emerged as the top TGF-β1-up-regulated miRNAs (Fig. 5C). qRT–PCR of the mature miRNAs and in situ hybridization experiments confirmed the microarray data (Fig. 5D) and showed that the observed up-regulation was time- and dose-dependent (Supplemental Fig. S5C). Induction of *miR-424(322)/503* was not restricted to MCF-10A cells, and, although it was less pronounced, we also observed induction in two additional nontransformed human cell lines (MCF-12A and 184B5), in primary HMECs (HuMECs), and in MMECs immortalized with TERT (Fig. 5E).

As mentioned above, TGF-β3 is a TGF-β ligand with a key role during involution (Nguyen and Pollard 2000). Thus, we also tested its ability to induce the expression of the miRNA cluster. Our data showed that comparable levels of *miR-424(322)* and *miR-503* up-regulation were induced with both TGF-β1 and TGF-β3 (Fig. 5F). Interestingly, none of the other *miR-16* family members were induced after TGF-β1 and TGF-β3 exposure.

To evaluate the role of the canonical TGF-β pathway in the regulation of *miR-424(322)/503*, we knocked down *SMAD4* before exposing MCF-10A cells to TGF-β1 (Fig. 5G). In knockdown cells, the induction of bona fide TGF-β targets such as *SMAD7*, *P21*, *CTCF*, *ATF3*, and *PAI-1* as well as *miR-424(322)* and *miR-503* was significantly reduced. Next we investigated which of the R-SMADs was involved in the regulation of *miR-424(322)/503*. Both SMAD2 and SMAD3 are activated during involution and when MCF-10A cells are exposed to TGF-β (Supplemental Fig. S5D). Thus, we individually silenced *SMAD2* and *SMAD3* (Supplemental Fig. S5E) and evaluated the up-regulation of the mature miR-423(322) and *miR-503* as well as the pri-miR cluster. Our studies clearly demonstrate that SMAD3 is the R-SMAD responsible for the up-regulation of the pri-*miR-424(322)/503* and the production of the miR mature forms upon TGF-β exposure (Supplemental Fig. S5F,G).

To further confirm the role of TGF-β in regulating the expression of *miR-424(322)/503*, we performed ChIP assays to investigate the presence of *SMAD4* in the endogenous putative promoter. To pursue this aim, we created a MCF-10A cell line where HA-tagged SMAD4 protein was constitutively expressed in MCF-10A cells. After ensuring that the exogenously introduced SMAD4 behaved as the endogenous protein did (both were shuttled into the nucleus in the presence of TGF-β) (Supplemental Fig. S6A), we used this cell line to perform ChIP with anti-HA antibodies. These studies revealed that SMAD4 was enriched in the putative *miR-424(322)/503* promoter after TGF-β exposure at levels comparable with the bona fide TGF-β target *PAI-1* (Fig. 6A). Importantly, the strongest enrichment happened in the region near the *SMAD4*-binding site.

To evaluate the role of the putative *SMAD4*-binding site in the up-regulation of the miRNA cluster upon TGF-β exposure, we first engineered a reporter construct containing an ~5.4-kb region upstream of the miRNA cluster followed by the *GFP* sequence (Fig. 6B). This reporter was integrated into the genome of MCF-10A cells by lentiviral delivery to create a pri-miR reporter cell line (MCF-10A-pri-miR-reporter). Reverse transcription using oligonucleotides complementary to *GFP* allowed us to study the transcript resulting exclusively from the reporter without interference of endogenous pri-miR (see the Materials and Methods). Upon addition of TGF-β to the MCF-10A-pri-miR-reporter cells, a clear increase in the transcription of the reporter was observed (Fig. 6C). Importantly, when we mutagenized the *SMAD4*-binding site, this increase was abrogated.

Next, we further characterized the pri-miR transcript controlled by this promoter. First, we identified the transcription start site (TSS) by performing 5′ rapid amplification of cDNA end (RACE). By using a specific primer located upstream of the miR cluster just before the region enriched in promoter-specific histone marks (~300 bp downstream from the *SMAD4*-binding site) for the reverse transcription step, we identified a TSS located downstream from the *E2F*-binding sites (Fig. 6D; Supplemental Fig. S6B). Interestingly, the addition of TGF-β shifted the TSS 181 nt upstream, which suggests the presence of an alternative promoter. As expected, we were able to amplify a region expanding from the miRNA cluster to the TSS by using overlapping PCRs (Supplemental Fig. S6C). qRT–PCR amplification and in situ hybridization confirmed the up-regulation of the pri-miRNA by TGF-β exposure (Fig. 6E; Supplemental Fig. S6C). As expected, the pri-miRNA was detected by in situ hybridization at the mammary epithelium of involuting mammary glands (3 d) (Supplemental Fig. S6D). Notably, kinetic studies of the pri-miRNA, pre-miRNA, and mature miRNA levels after addition of TGF-β revealed that

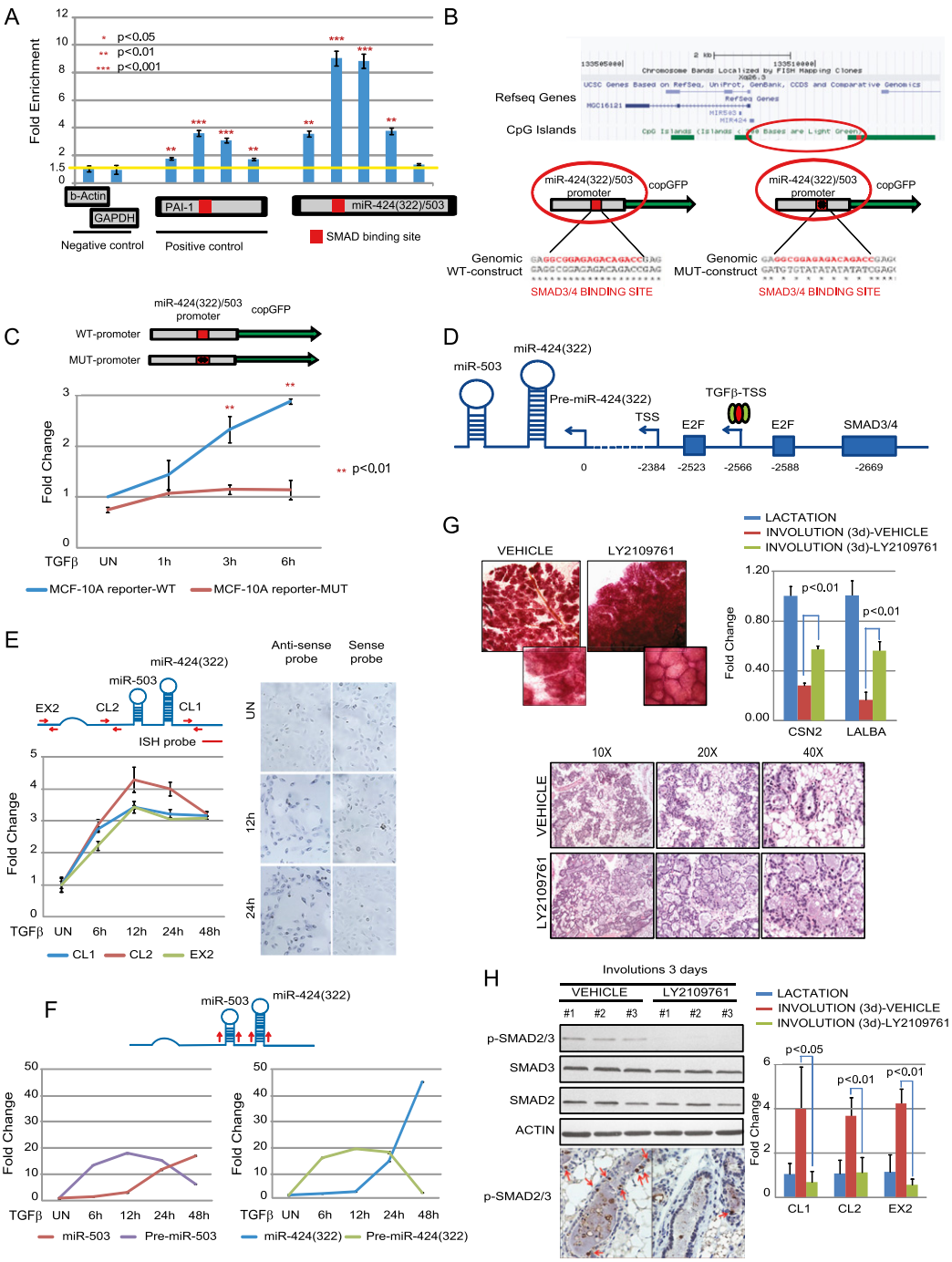

Figure 6. Characterization of the *miR-424(322)/503* promoter, pri-*miR-424(322)/503*, and transcriptional regulation by TGF-β in vivo. (*A*) MCF-10A cells stably expressing HA-tagged SMAD4 or a control empty vector were treated with 10 ng/mL TGF-β for 3 h, and ChIP was performed using an anti-HA antibody. The quantification of genomic DNA enrichment was performed using specific primers surrounding the promoter. The putative *SMAD*-binding site is indicated by a red square. Quantification of DNA enrichment in the *PAI-1* gene promoter was used as a positive control, while β-Actin and Gapdh were used as negative controls. (*B*) A schematic illustration obtained from the UCSC genome database showing the localization of *miR-424(322)* and *miR-503* and the upstream putative 5.4-kb promoter region containing either the wild-type or mutated *SMAD*-binding site that was cloned into a reporter vector, as explained in the text. (*C*) MCF-10A cells were transduced with either the wild-type or mutated promoters and treated with or without 10 ng/mL TGF-β, and the promoter activity was analyzed by qRT–PCR. (*D*) Representation of the proposed *miR-424(322)/503* cluster promoter region containing the *SMAD*-binding site and the alternative TSSs identified by 5′ RACE in the presence and absence of TGF-β. (*E*) Expression kinetics of pri-*miR-424(322)/503* after treatment of MCF-10A cells with 10 ng/mL TGF-β for the specified time points by qRT–PCR using specific primers surrounding the pre-*miR-424(322)* and pre-*miR-503* (*left*) or by in situ hybridization using a probe against pri-*miR-424(322)/503* (*right*). (*F*) qRT–PCR analysis showing that increased mature *miR-424(322)* and *miR-503* levels after treatment of MCF-10A cells with 10 ng/mL TGF-β coincide with a decrease in pre-*miR-424(322)* and pre-*miR-503*, respectively. (*G*) After inhibition of TGF-β signaling in vivo by the administration of the specific inhibitor LY2109761, mammary glands were examined 72 h after weaning for the presence of secretory acini by H&E and for epithelial density by whole-mount carmine red staining. Additionally, mammary epithelial cells were purified, and milk protein production was evaluated by qRT–PCR using specific primers for α-lactalbumin and β-casein genes. (*H*) Inhibition of the activation of the TGF-β pathway, shown by Western blot and immunohistochemistry for activated phospho-SMAD2/3, abrogates the transcription of pri-*miR-424(322)/503* during involution, as shown by qRT–PCR. See also Supplemental Figure S6, E and F, for a similar study using the TGF-β inhibitor LY2157299.

the increase in pri-miRNA and pre-miRNA happens first and that generation of mature miRNAs leads to a reduction of the pri-miRNA and pre-miRNA (Fig. 6E,F). This could be due to the cleavage and degradation of the pri-miRNA after the pre-miRNA is excised, the existence of a negative regulatory feedback loop, or a combination of both mechanisms.

Finally, to test that the regulation of *miR-424(322)/503* by TGF-β occurs in vivo during involution, we individually treated lactating females with two different specific inhibitors of TGF-β receptor I and II with demonstrated activity in vivo (LY2109761 and LY2157299) (Melisi et al. 2008; Bouquet et al. 2011; Calon et al. 2012; Bhola et al. 2013) and analyzed the induction of the miR cluster. When lactating females were pretreated with these inhibitors starting 24 h before weaning, these animals showed an evident inhibition of involution 3 d after weaning, as indicated by carmine red and H&E staining of the mammary gland and qRT–PCR levels of milk proteins (Fig. 6G; Supplemental Fig. S6E). Importantly, due to the inhibition of TGF-β signaling, they also presented a strong reduction in the levels of pri-*miR-424(322)/503* (Fig. 6H; Supplemental Fig. S6F).

Discussion

Despite the established role of a variety of extrinsic and intrinsic signals regulating mammary gland development (Howard and Gusterson 2000; Macias and Hinck 2012), a restricted number of studies have identified and validated miRNAs with a role in any aspect of normal mammary gland biology (Avril-Sassen et al. 2009; Tanaka et al. 2009; Ucar et al. 2010; Yang et al. 2010; Cui et al. 2011; Le Guillou et al. 2012), and even fewer have studied their function using transgenic animal models (Ucar et al. 2010; Le Guillou et al. 2012). Here we unveiled the miRNA cluster *miR-424(322)/503* as an important regulator of the massive reorganization that occurs in the mammary epithelium after pregnancy. Furthermore, through the generation of a knockout mouse model, we characterized mechanistically its role and regulation.

Among the 12 identified miRNAs, *miR-424(322)* showed the largest fold increase between lactation and involution. Although this miRNA has been studied in the context of monocyte differentiation (Rosa et al. 2007; Forrest et al. 2010) and endothelial cell regulation (Ghosh et al. 2010; Nakashima et al. 2010; Kim et al. 2013), a potential role in mammary epithelial architecture remodeling has not yet been described. The characterization of the mammary epithelium of *miR-424(322)/503* knockout females during development revealed a defect during involution. To understand the role of *miR-424(322)/503* in this biological context, we considered two pertinent questions: (1) Which are the relevant targets modulated by the cluster in the mammary epithelium? (2) How is the pri-miR regulated?

Through our comprehensive studies in vitro and in vivo, we identified *BCL-2* and *IGF1R* as robust target genes of the *miR-424(322)/503* cluster in the mammary epithelium. Interestingly, our data did not validate previous data reporting *CCNE1* as a target of this miRNA cluster (Forrest et al. 2010; Nakashima et al. 2010). Since the relevance of the different miRNA targets is context-dependent (Liu and Kohane 2009; Inui et al. 2010), it is important to mention that we used HMECs for our studies and achieved mature miRNA expression levels comparable with the observed during involution in vivo. Notably, when we augmented by lentiviral transduction the intracellular levels of the mature miRNAs several fold (>10 times) over the levels found in vivo, we observed a reliable reduction of CCNE1 protein (Supplemental Fig. S3F). Finally, no major changes were observed in CCNE1 protein levels from lactation to involution. Thus, our data illustrate the importance of the biological context in identifying relevant miRNA targets for different processes, and, consequently, we do not consider CCNE1 a relevant target of the *miR-424(322)/503* in the context of mammary epithelial involution and TGF-β exposure.

During the last two decades, key details about the mechanism and regulation of mammary gland involution have been identified (Stein et al. 2007). The use of genetically modified mice with gain or loss of function has provided evidence regarding the implication of *Bcl-2* and *Igf1r* in this process. The Igf1/Igf1r axis plays critical roles in multiple steps of mammary development (Hynes and Watson 2010). During involution, IGF signaling has been found to be inhibited by down-regulation of Igf1r (Modha et al. 2004) and up-regulation of insulin-like growth factor-binding protein 5 (Igfbp-5) (Allan et al. 2004). Importantly, the effect of IGF signaling in life or death fate decisions has been related to its effect on the PI3K–AKT/PKB and the Ras–MAPK pathways (Allan et al. 2004; Stein et al. 2007). In accordance with this, involution has been found to be inhibited in transgenic animals with constitutively active *Akt* (Schwertfeger et al. 2001; Ackler et al. 2002). BCL-2 family members are also involved in regulating cellular fate after the pregnancy cycle (Colitti 2012). Levels of proapoptotic Bak and Bad increase during lactation, reaching their peak during involution. In contrast, anti-apoptotic Bcl-W and Bcl-2 are strongly down-regulated at the onset of apoptosis (Metcalfe et al. 1999). In the proposed model, mammary epithelial cells are poised for apoptosis with higher levels of the death effectors but are prevented from triggering apoptosis by anti-apoptotic Bcl-2 family proteins until involution, when prosurvival gene expression levels decline (Metcalfe et al. 1999; Stein et al. 2007; Colitti 2012). In agreement with this view, enforced expression of *Bak* induces rapid mammary apoptosis (Metcalfe et al. 1999), while high levels of *Bcl-2* have been shown to potently regulate mammary epithelial cell survival and inhibit alveolar cell apoptosis during involution (Jager et al. 1997; Schorr et al. 1999).

By understanding the signals that initiate the transcriptional up-regulation of the miR cluster, we uncovered its regulation by TGF-β. As TGF-β ligands have well-known roles in epithelial mammary gland morphogenesis (Nguyen and Pollard 2000; Stein et al. 2007), this information provided us with a potential link between the induction

of involution and the up-regulation of the miR cluster. It is interesting to discuss that the R-SMAD that controls the up-regulation of the *miR-424(322)/503*, SMAD3, has been found to control not only transcription but also miRNA processing in a SMAD4-independent function (Davis et al. 2008, 2010). Thus, a question is whether this also applies for the production of mature *miR-424(322)* and *miR-503*. SMAD3 has been found to interact with DROSHA and affect miRNA maturation by binding to a conserved 5-base motif (SBE; 5′-CAGAC-3′) present in the pri-miRs. However the pri-*miR-424(322)/503* cluster transcript does not contain this binding element. Additionally, individual silencing of both *SMAD3* and *SMAD4* completely abrogated the up-regulation of both pri-*miR-424(322)/503* and individual mature forms. Thus, at this point, transcriptional up-regulation seems to be a critical step, and additional studies will be required to clarify a potential miRNA processing function of pri-*miR-424(322)/503* by SMAD3.

Mechanistically, our data suggest a model (Fig. 7) in which milk stasis after weaning rapidly induces the expression of TGF-β3. Activation of the TGF-β pathway induces the transcription of pri-*miR-424(322)/503*. This primary transcript is processed to preferentially generate mature *miR-424(322)*, which in turn down-regulates the expression of components of the involution response, *IGF1R* and *BCL-2*. Our data have unveiled a previously unknown multilayered regulation of epithelial tissue remodeling coordinated by the miRNA cluster *miR-424(322)/503*.

Our work may also have implications regarding tumor biology because several members of the *miR-16* family have been involved in human malignancies (Liu et al. 2008; Aqeilan et al. 2010). All *miR-424(322)/503* targets studied here have been shown to be associated with human cancers as oncogenes (Yip and Reed 2008; Pollak 2012). The ability of *miR-424(322)/503* to modulate target expression raises the question of whether it is also

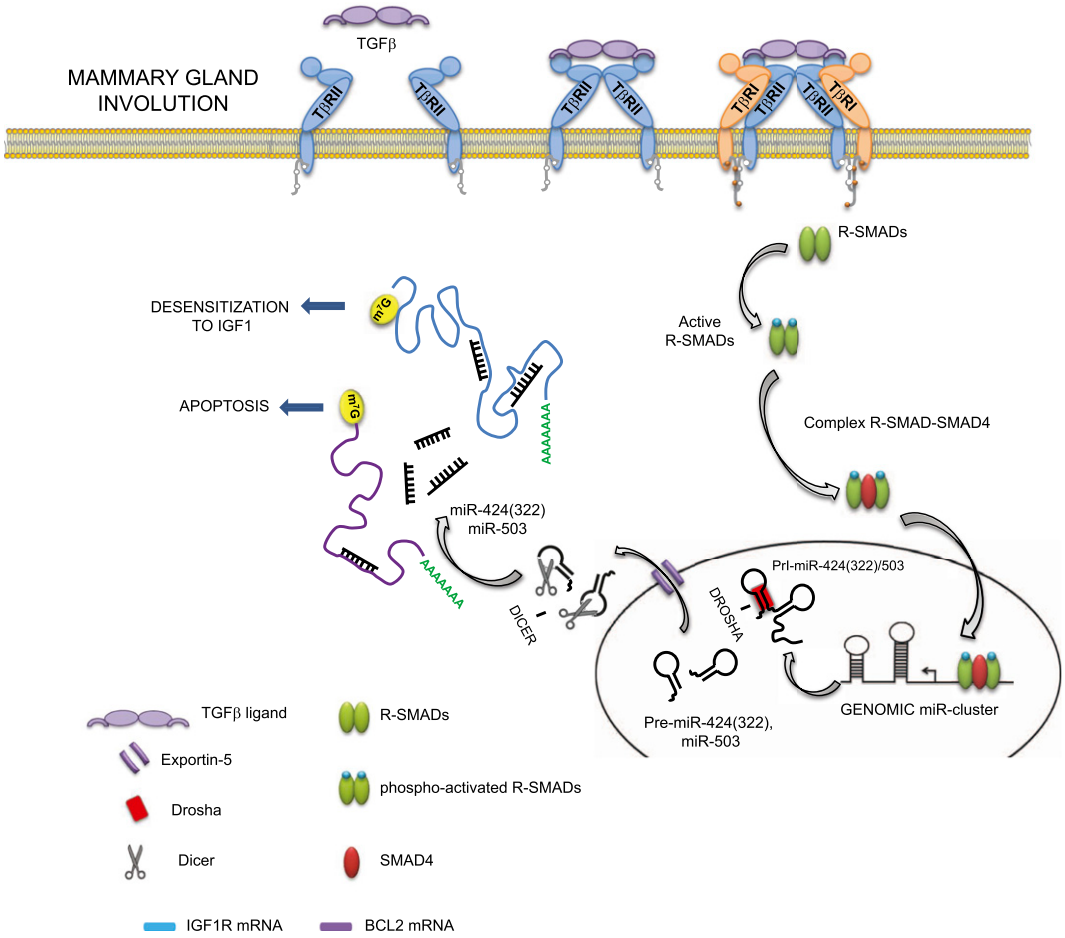

Figure 7. Proposed mechanistic model of *miR-424(322)/503* function. During mammary gland involution, critical events dictate the reorganization of the mammary epithelial cell compartment. TGF-β, a well-known player, governs involution in part by inducing the expression of a miRNA primary transcript containing the *miR-424(322)/503* cluster. The generation of the mature miRNAs, mainly *miR-424(322)*, reduces the expression of targets such as *IGF1R* and *BCL2*. This reduction results in attenuation of IGF signaling and sensitization to apoptosis, leading the epithelial cells toward cell death during involution. The above highlights the *miR-424(322)/503* cluster as a critical regulator of mammary gland homeostasis through its ability to dictate cell life and death decisions through balancing proliferation, survival, and cell death pathways.

involved in breast tumorigenesis. Our data in this regard reveal that knockout animals accumulate alveoli hyperplasia, but we did not observe tumor development in animals followed up to 1 yr of age. Longer periods of follow-up, multiple pregnancies, or both may be necessary to generate full cell transformation in these animals. Interestingly, *miR-424(322)/503* is located in a chromosomal region that has been recently identified to present significant deletions in ~8% of hormone receptor-positive breast cancers (Dvinge et al. 2013). Furthermore, the promoter region that we identified is placed on a CpG island that could be targeted by hypermethylation as a potential mechanism to down-regulate the expression of the miRNAs during transformation. As *miR-424(322)/503* is located in the silenced part of the X chromosome, a single inactivation event is enough to fully abrogate its expression. Interestingly, it has been recently reported that suppressed *miR-424(322)* expression contributes to the progression of cervical cancer (Xu et al. 2013). Additional research will be necessary to fully define the potential role of *miR-424(322)/503* in breast tumorigenesis. In this regard, our work describing the biological role of *miR-424(322)/503* during involution and its regulation establishes the basis for future studies.

Materials and methods

Cell culture

Cell lines were obtained from the American Type Culture Collection. Normal breast epithelial MCF-10A and MCF-12 cells were cultured at 37°C/5%CO_2 in DMEM/Ham's F-12 supplemented with 10% penicillin/streptomycin, 20 ng/mL EGF, 10 μg/mL insulin, 100 ng/mL cholera toxin, 500 ng/mL hydrocortisone, and 5% horse serum. HuMECs (Life Technologies, no. A10565) were grown according to instructions and reagents provided by the manufacturer. 184B5 cells were grown in MEGM medium (Lonza/Clonetics, no. CC-3150) supplemented with 1 ng/mL cholera toxin. Phoenix cells were grown in DMEM–10% fetal bovine serum and 10% penicillin/streptomycin at 37°C/5%CO_2.

TGFβ1 and TGFβ3 were purchased from Sigma (nos. T7039 and T5425, respectively). Human recombinant IGF1 was purchased from PROSPEC (no. CYT-216). Cisplatin (no. P4394) and paclitaxel (no. T7402) were both from Sigma.

miRNA extraction and HTP-seq

To perform mature miRNA and pre-miRNA expression analysis by qRT–PCR, RNA was purified using the miRVANA miRNA isolation kit (Ambion, no. AM1561) according to the instructions provided. Reverse transcription was performed on 50 ng of RNA using the miRNA reverse transcription kit (Roche, no. 4366596). miRNA deep sequencing was conducted at the Columbia University Genome Center's core facility (http://genomecenter.columbia.edu) using the Illumina platform. RNA sequencing (RNA-seq) was performed at HiSeq single reads with a depth of coverage of 20 million reads per sample.

Luciferase reporter assays

3′ UTRs of specific target genes were cloned downstream from the luciferase reporter in the pMIR-REPORT vector (Life Technologies, no. AM5795M) by PCR from human genomic DNA using restriction enzymes. Relative luciferase units (RLUs) were measured using the Dual-Glo luciferase assay system (Promega, no. E2949). For a detailed description, see the Supplemental Material.

Mouse generation and LY2109761 treatment

To generate single *miR-424(322)* and *miR-503* or double-knockout mice, we used ZNF (Sigma; for a detailed description, see the Supplemental Material). To inhibit TGF-β signaling during involution, lactating wild-type and *miR-424(322)*$^{-/-}$/*miR-503*$^{-/-}$ double-knockout females were pretreated by oral gavage twice daily with 50 mg/kg LY2109761 (Selleckchem) for 24 h before weaning. Thereafter, mice were treated again by oral gavage twice daily with 50 mg/kg LY2109761 for 1 and 3 d. Mice were sacrificed, and mammary glands were dissected as mentioned previously. All experiments were performed under the Institutional Animal Care and Use Committee (IACUC) guidelines.

PAR-CLIP analysis

A PAR-CLIP assay to measure AGO2 enrichment in *miR-424(322)/503* mRNA targets was performed as described previously (Hafner et al. 2010). Briefly, cells were pretreated with 50 μM 4-thiouridine (Sigma, no. T4509) overnight and cross-linked at 150 mJ/cm^2 at 365 nm UV on ice. Immunoprecipitation was performed using an anti-AGO2 antibody (Abnova, no. H00027161-M01) overnight at 4°C. RNA was extracted using the miRVANA miRNA isolation kit, and retrotranscribed RNA was subjected to analysis by qRT–PCR using specific primers.

Quantification of the number of miR-424(322) *and* miR-503 *molecules*

The number of molecules was estimated using chemically synthesized RNA oligonucleotides that mimic in sequence *miR-424(322)* and *miR-503*. RNA oligonucleotides were prepared in serial dilutions corresponding to 1 pg of miRNA per microliter, 0.1 pg of miRNA per microliter, 0.01 pg of miRNA per microliter, and 1 fg of miRNA per microliter. One microliter of each dilution was retrotranscribed in parallel with 50 ng of our samples. The number of molecules per cell was estimated by considering a ratio of 10 pg of RNA per cell and integrating the experimental Ct values into the standard values obtained with the commercial oligonucleotides.

Flow cytometry and cell viability

All flow cytometry experiments were performed on a BD FacsCalibur cell analyzer using the CellQuest Pro software on Mac OSX. To analyze apoptosis induced by cisplatin and paclitaxel, we performed the Annexin-V staining following the FITC Annexin-V apoptosis detection kit guidelines (BD Pharmingen, no. 556570). For a detailed description, see the Supplemental Material.

Whole-mount preparations and immunohistochemistry

To prepare whole-mount carmine red staining, mammary glands were fixed in 4% paraformaldehyde for 1 h, stained with carmine red (Sigma, no. C1022) overnight at room temperature, and ultimately dehydrated and fixed in xilol. To perform immunohistochemical analysis, formalin-fixed paraffin-embedded samples were deparaffinized and rehydrated. Peroxidase inactivation and antigen retrieval were achieved by incubating samples in 1%

H_2O_2 and citric buffer. The antibodies used were Ki67 (1:200; Abcam, no. ab15580), anti-cytokeratin 18 antibody (1:300; Abcam, no. ab668), anti-cytokeratin 5 (1:1000; Covance, no. PRB-160P), cleaved caspase-3 (1:500; Cell Signaling, no. 9664), and p-SMAD2/3 (1:100; Cell Signaling, no. 9510).

Gene expression and miRNA expression arrays

For gene expression and miRNA expression arrays, MCF-10A cells were treated with TGFβ, and RNA was extracted using RNeasy and miRVANA extraction kits, respectively, and labeled using the LowInput QuickAmp labeling kit (Agilent, no. 5190-2331). RNAs were hybridized on a human GE 4x44K v2 microarray kit (Agilent, no. G4845A) and a human miRNA V2 oligo microarray (Agilent, no. G4470B), respectively. Gene expression array data have been uploaded and are available in the Gene Expression Omnibus database.

ChIP

MCF-10A untreated and TGFβ cells were cross-linked with 11% formaldehyde solution for 10 min at room temperature, lysed, and sonicated using a Bioruptor Standard sonication device (Diagenode, no. UCD-200 TM; see the Supplemental Material). HA-SMAD4 immunoprecipitation was performed using the DynaMag-2 magnetic particle concentrator (Invitrogen, no. 123.21D), protein G Dynabeads (Invitrogen, no. 100.03D), and an anti-HA antibody (Roche, no. 11867423001) overnight at 4°C on a rotator. Thereafter, samples were collected and washed, and phenol/chloroform/isoamyl alcohol extraction using Phaselock tubes (Prime, no. 2302840) was performed to isolate DNA. DNA enrichment was analyzed by qRT–PCR using specific primers. Data are presented as the Δ-normalized values between SMAD4-HA [Δ (TGFβ-treated) − (untreated)] − EV [Δ (TGFβ-treated) − (untreated)]. For a detailed description, see the Supplemental Material.

In situ hybridization

Briefly, probes against pri-hsa-*miR-424(322)/503* were created from human genomic DNA by PCR using specific oligonucleotides and were obtained by T7-driven in vitro RNA synthesis. Probes against mature *miR-424(322)* and *miR-503* were purchased from Exiqon (catalog no. 38195-08), and the assay was visualized using a tyramide signal amplification method (PerkinElmer, NEL741001KT). For a detailed description, see the Supplemental Material.

References

Ackler S, Ahmad S, Tobias C, Johnson MD, Glazer RI. 2002. Delayed mammary gland involution in MMTV–AKT1 transgenic mice. *Oncogene* **21:** 198–206.

Ahn HW, Morin RD, Zhao H, Harris RA, Coarfa C, Chen ZJ, Milosavljevic A, Marra MA, Rajkovic A. 2010. MicroRNA transcriptome in the newborn mouse ovaries determined by massive parallel sequencing. *Mol Hum Reprod* **16:** 463–471.

Allan GJ, Beattie J, Flint DJ. 2004. The role of IGFBP-5 in mammary gland development and involution. *Domest Anim Endocrinol* **27:** 257–266.

Aqeilan RI, Calin GA, Croce CM. 2010. miR-15a and miR-16-1 in cancer: discovery, function and future perspectives. *Cell Death Differ* **17:** 215–220.

Avril-Sassen S, Goldstein LD, Stingl J, Blenkiron C, Le Quesne J, Spiteri I, Karagavriilidou K, Watson CJ, Tavare S, Miska EA, et al. 2009. Characterisation of microRNA expression in post-natal mouse mammary gland development. *BMC Genomics* **10:** 548.

Bartel DP. 2004. MicroRNAs: genomics, biogenesis, mechanism, and function. *Cell* **116:** 281–297.

Bartel DP. 2009. MicroRNAs: target recognition and regulatory functions. *Cell* **136:** 215–233.

Bernstein BE, Mikkelsen TS, Xie X, Kamal M, Huebert DJ, Cuff J, Fry B, Meissner A, Wernig M, Plath K, et al. 2006. A bivalent chromatin structure marks key developmental genes in embryonic stem cells. *Cell* **125:** 315–326.

Bhola NE, Balko JM, Dugger TC, Kuba MG, Sanchez V, Sanders M, Stanford J, Cook RS, Arteaga CL. 2013. TGF-β inhibition enhances chemotherapy action against triple-negative breast cancer. *J Clin Invest* **123:** 1348–1358.

Bouquet F, Pal A, Pilones KA, Demaria S, Hann B, Akhurst RJ, Babb JS, Lonning SM, DeWyngaert JK, Formenti SC, et al. 2011. TGFβ1 inhibition increases the radiosensitivity of breast cancer cells in vitro and promotes tumor control by radiation in vivo. *Clin Cancer Res* **17:** 6754–6765.

Calon A, Espinet E, Palomo-Ponce S, Tauriello DV, Iglesias M, Cespedes MV, Sevillano M, Nadal C, Jung P, Zhang XH, et al. 2012. Dependency of colorectal cancer on a TGF-β-driven program in stromal cells for metastasis initiation. *Cancer Cell* **22:** 571–584.

Chapman RS, Lourenco PC, Tonner E, Flint DJ, Selbert S, Takeda K, Akira S, Clarke AR, Watson CJ. 1999. Suppression of epithelial apoptosis and delayed mammary gland involution in mice with a conditional knockout of Stat3. *Genes Dev* **13:** 2604–2616.

Colitti M. 2012. BCL-2 family of proteins and mammary cellular fate. *Anat Histol Embryol* **41:** 237–247.

Cui W, Li Q, Feng L, Ding W. 2011. MiR-126-3p regulates progesterone receptors and involves development and lactation of mouse mammary gland. *Mol Cell Biochem* **355:** 17–25.

Davis BN, Hilyard AC, Lagna G, Hata A. 2008. SMAD proteins control DROSHA-mediated microRNA maturation. *Nature* **454:** 56–61.

Davis BN, Hilyard AC, Nguyen PH, Lagna G, Hata A. 2010. Smad proteins bind a conserved RNA sequence to promote microRNA maturation by Drosha. *Mol Cell* **39:** 373–384.

Dvinge H, Git A, Graf S, Salmon-Divon M, Curtis C, Sottoriva A, Zhao Y, Hirst M, Armisen J, Miska EA, et al. 2013. The shaping and functional consequences of the microRNA landscape in breast cancer. *Nature* **497:** 378–382.

Faure E, Heisterkamp N, Groffen J, Kaartinen V. 2000. Differential expression of TGF-β isoforms during postlactational mammary gland involution. *Cell Tissue Res* **300:** 89–95.

Finnerty JR, Wang WX, Hebert SS, Wilfred BR, Mao G, Nelson PT. 2010. The miR-15/107 group of microRNA genes: evolutionary biology, cellular functions, and roles in human diseases. *J Mol Biol* **402:** 491–509.

Forrest AR, Kanamori-Katayama M, Tomaru Y, Lassmann T, Ninomiya N, Takahashi Y, de Hoon MJ, Kubosaki A, Kaiho A, Suzuki M, et al. 2010. Induction of microRNAs, mir-155, mir-222, mir-424 and mir-503, promotes monocytic differentiation through combinatorial regulation. *Leukemia* **24:** 460–466.

Ghosh G, Subramanian IV, Adhikari N, Zhang X, Joshi HP, Basi D, Chandrashekhar YS, Hall JL, Roy S, Zeng Y, et al. 2010. Hypoxia-induced microRNA-424 expression in human endothelial cells regulates HIF-α isoforms and promotes angiogenesis. *J Clin Invest* **120:** 4141–4154.

Gorska AE, Jensen RA, Shyr Y, Aakre ME, Bhowmick NA, Moses HL. 2003. Transgenic mice expressing a dominant-negative mutant type II transforming growth factor-β receptor

exhibit impaired mammary development and enhanced mammary tumor formation. *Am J Pathol* **163:** 1539–1549.
Grimson A, Farh KK, Johnston WK, Garrett-Engele P, Lim LP, Bartel DP. 2007. MicroRNA targeting specificity in mammals: determinants beyond seed pairing. *Mol Cell* **27:** 91–105.
Guo H, Ingolia NT, Weissman JS, Bartel DP. 2010. Mammalian microRNAs predominantly act to decrease target mRNA levels. *Nature* **466:** 835–840.
Hafner M, Landthaler M, Burger L, Khorshid M, Hausser J, Berninger P, Rothballer A, Ascano M Jr, Jungkamp AC, Munschauer M, et al. 2010. Transcriptome-wide identification of RNA-binding protein and microRNA target sites by PAR-CLIP. *Cell* **141:** 129–141.
Howard BA, Gusterson BA. 2000. Human breast development. *J Mammary Gland Biol Neoplasia* **5:** 119–137.
Hynes NE, Watson CJ. 2010. Mammary gland growth factors: roles in normal development and in cancer. *Cold Spring Harb Perspect Biol* **2:** a003186.
Iavarone A, Massague J. 1997. Repression of the CDK activator Cdc25A and cell-cycle arrest by cytokine TGF-β in cells lacking the CDK inhibitor p15. *Nature* **387:** 417–422.
Inui M, Martello G, Piccolo S. 2010. MicroRNA control of signal transduction. *Nat Rev Mol Cell Biol* **11:** 252–263.
Ip MM, Asch BB. 2000. Introduction: an histology atlas of the rodent mammary gland and human breast during normal postnatal development and in cancer. *J Mammary Gland Biol Neoplasia* **5:** 117–118.
Jager R, Herzer U, Schenkel J, Weiher H. 1997. Overexpression of Bcl-2 inhibits alveolar cell apoptosis during involution and accelerates c-myc-induced tumorigenesis of the mammary gland in transgenic mice. *Oncogene* **15:** 1787–1795.
Johnson K, Kirkpatrick H, Comer A, Hoffmann FM, Laughon A. 1999. Interaction of Smad complexes with tripartite DNA-binding sites. *J Biol Chem* **274:** 20709–20716.
Karakas B, Weeraratna A, Abukhdeir A, Blair BG, Konishi H, Arena S, Becker K, Wood W 3rd, Argani P, De Marzo AM, et al. 2006. Interleukin-1α mediates the growth proliferative effects of transforming growth factor-β in p21 null MCF-10A human mammary epithelial cells. *Oncogene* **25:** 5561–5569.
Kim J, Kang Y, Kojima Y, Lighthouse JK, Hu X, Aldred MA, McLean DL, Park H, Comhair SA, Greif DM, et al. 2013. An endothelial apelin-FGF link mediated by miR-424 and miR-503 is disrupted in pulmonary arterial hypertension. *Nat Med* **19:** 74–82.
Le Guillou S, Sdassi N, Laubier J, Passet B, Vilotte M, Castille J, Laloe D, Polyte J, Bouet S, Jaffrezic F, et al. 2012. Overexpression of miR-30b in the developing mouse mammary gland causes a lactation defect and delays involution. *PLoS ONE* **7:** e45727.
Lewis BP, Burge CB, Bartel DP. 2005. Conserved seed pairing, often flanked by adenosines, indicates that thousands of human genes are microRNA targets. *Cell* **120:** 15–20.
Liu H, Kohane IS. 2009. Tissue and process specific microRNA–mRNA co-expression in mammalian development and malignancy. *PLoS ONE* **4:** e5436.
Liu Q, Fu H, Sun F, Zhang H, Tie Y, Zhu J, Xing R, Sun Z, Zheng X. 2008. miR-16 family induces cell cycle arrest by regulating multiple cell cycle genes. *Nucleic Acids Res* **36:** 5391–5404.
Macias H, Hinck L. 2012. Mammary gland development. *Wiley Interdiscip Rev Dev Biol* **1:** 533–557.
Massague J, Seoane J, Wotton D. 2005. Smad transcription factors. *Genes Dev* **19:** 2783–2810.
Melisi D, Ishiyama S, Sclabas GM, Fleming JB, Xia Q, Tortora G, Abbruzzese JL, Chiao PJ. 2008. LY2109761, a novel transforming growth factor β receptor type I and type II dual inhibitor, as a therapeutic approach to suppressing pancreatic cancer metastasis. *Mol Cancer Ther* **7:** 829–840.
Metcalfe AD, Gilmore A, Klinowska T, Oliver J, Valentijn AJ, Brown R, Ross A, MacGregor G, Hickman JA, Streuli CH. 1999. Developmental regulation of Bcl-2 family protein expression in the involuting mammary gland. *J Cell Sci* **112:** 1771–1783.
Modha G, Blanchard A, Iwasiow B, Mao XJ, Troup S, Adeyinka A, Watson P, Shiu R, Myal Y. 2004. Developmental changes in insulin-like growth factor I receptor gene expression in the mouse mammary gland. *Endocr Res* **30:** 127–140.
Nakashima T, Jinnin M, Etoh T, Fukushima S, Masuguchi S, Maruo K, Inoue Y, Ishihara T, Ihn H. 2010. Down-regulation of mir-424 contributes to the abnormal angiogenesis via MEK1 and cyclin E1 in senile hemangioma: its implications to therapy. *PLoS ONE* **5:** e14334.
Neuenschwander S, Schwartz A, Wood TL, Roberts CT Jr, Hennighausen L, LeRoith D. 1996. Involution of the lactating mammary gland is inhibited by the IGF system in a transgenic mouse model. *J Clin Invest* **97:** 2225–2232.
Nguyen AV, Pollard JW. 2000. Transforming growth factor β3 induces cell death during the first stage of mammary gland involution. *Development* **127:** 3107–3118.
Pollak M. 2012. The insulin and insulin-like growth factor receptor family in neoplasia: an update. *Nat Rev Cancer* **12:** 159–169.
Pollard KS, Hubisz MJ, Rosenbloom KR, Siepel A. 2010. Detection of nonneutral substitution rates on mammalian phylogenies. *Genome Res* **20:** 110–121.
Rissland OS, Hong SJ, Bartel DP. 2011. MicroRNA destabilization enables dynamic regulation of the miR-16 family in response to cell-cycle changes. *Mol Cell* **43:** 993–1004.
Rosa A, Ballarino M, Sorrentino A, Sthandier O, De Angelis FG, Marchioni M, Masella B, Guarini A, Fatica A, Peschle C, et al. 2007. The interplay between the master transcription factor PU.1 and miR-424 regulates human monocyte/macrophage differentiation. *Proc Natl Acad Sci* **104:** 19849–19854.
Schorr K, Li M, Bar-Peled U, Lewis A, Heredia A, Lewis B, Knudson CM, Korsmeyer SJ, Jager R, Weiher H, et al. 1999. Gain of Bcl-2 is more potent than bax loss in regulating mammary epithelial cell survival in vivo. *Cancer Res* **59:** 2541–2545.
Schwertfeger KL, Richert MM, Anderson SM. 2001. Mammary gland involution is delayed by activated Akt in transgenic mice. *Mol Endocrinol* **15:** 867–881.
Shirdel EA, Xie W, Mak TW, Jurisica I. 2011. NAViGaTing the micronome—using multiple microRNA prediction databases to identify signalling pathway-associated microRNAs. *PLoS ONE* **6:** e17429.
Stein T, Salomonis N, Gusterson BA. 2007. Mammary gland involution as a multi-step process. *J Mammary Gland Biol Neoplasia* **12:** 25–35.
Tanaka T, Haneda S, Imakawa K, Sakai S, Nagaoka K. 2009. A microRNA, miR-101a, controls mammary gland development by regulating cyclooxygenase-2 expression. *Differentiation* **77:** 181–187.
Tiffen PG, Omidvar N, Marquez-Almuina N, Croston D, Watson CJ, Clarkson RW. 2008. A dual role for oncostatin M signaling in the differentiation and death of mammary epithelial cells in vivo. *Mol Endocrinol* **22:** 2677–2688.
Ucar A, Vafaizadeh V, Jarry H, Fiedler J, Klemmt PA, Thum T, Groner B, Chowdhury K. 2010. miR-212 and miR-132 are required for epithelial stromal interactions necessary for mouse mammary gland development. *Nat Genet* **42:** 1101–1108.

Urnov FD, Rebar EJ, Holmes MC, Zhang HS, Gregory PD. 2010. Genome editing with engineered zinc finger nucleases. *Nat Rev Genet* **11:** 636–646.

Watson CJ. 2006. Post-lactational mammary gland regression: molecular basis and implications for breast cancer. *Expert Rev Mol Med* **8:** 1–15.

Watson CJ, Kreuzaler PA. 2011. Remodeling mechanisms of the mammary gland during involution. *Int J Dev Biol* **55:** 757–762.

Xu J, Li Y, Wang F, Wang X, Cheng B, Ye F, Xie X, Zhou C, Lu W. 2013. Suppressed miR-424 expression via upregulation of target gene Chk1 contributes to the progression of cervical cancer. *Oncogene* **32:** 976–987.

Yang X, Lin X, Zhong X, Kaur S, Li N, Liang S, Lassus H, Wang L, Katsaros D, Montone K, et al. 2010. Double-negative feedback loop between reprogramming factor LIN28 and microRNA let-7 regulates aldehyde dehydrogenase 1-positive cancer stem cells. *Cancer Res* **70:** 9463–9472.

Yip KW, Reed JC. 2008. Bcl-2 family proteins and cancer. *Oncogene* **27:** 6398–6406.